Applied Catalysis A, General 554 (2018) 64–70

Contents lists available at ScienceDirect

Applied Catalysis A, General

journal homepage: www.elsevier.com/locate/apcata

Hydrothermal modification of the alumina catalyst for the skeletal isomerization of n-butenes

Ildar N. Mukhambetov[a], Svetlana R. Egorova[b,*], Aliya N. Mukhamed'yarova[b], Alexander A. Lamberov[b]

[a] Mirrico Group of Companies, St. Ostrovskogo, 84, 420107, Kazan, Russian Federation
[b] Alexander Butlerov Institute of Chemistry, Kazan Federal University, St. Kremlin, 29/1, 420008, Kazan, Russian Federation

ARTICLE INFO

Keywords:
Alumina catalyst
Skeletal isomerization of n-butenes
Hydrothermal treatment

ABSTRACT

Hydrothermal modification of the alumina catalyst of n-butenes skeletal isomerization was investigated. It is shown that during the hydrothermal treatment of γ-Al_2O_3 and subsequent calcination its activity in skeletal isomerization of n-butenes first increases, and then it decreases with a rise of the hydrothermal treatment duration. This behavior is due to a similar change in the content of the strong Lewis acid sites of alumina, which are the active centers of reaction and they can be identified by IR-spectroscopy of the adsorbed pyridine and EPR-spectroscopy of the adsorbed anthraquinone. We report the mechanism of new Lewis acid sites formation at the γ-Al_2O_3 hydrothermal treatment containing X-ray amorphous component.

1. Introduction

Active aluminum oxide (γ-Al_2O_3) is most often used in a series of oxide catalysts and catalyst carriers due to a unique combination of thermal stability, mechanical strength, developed surface and acid-base properties. Its acid properties affect the dispersity of the active component in the catalyst; the acid sites are the active centers in dehydration and isomerization reactions; they are also involved in oligomerization of hydrocarbons [1–10].

The skeletal isomerization of n-butenes (1-butene, trans-2-butene, cis-2-butene) to 2-methylpropene proceeds on the Lewis acid sites of γ-Al_2O_3 by the carbon-ion mechanism, including the stages of n-butene adsorption with formation of carbonium ion of linear structure, its isomerization to the tertiary ion, and desorption of 2-methylpropene [11]. Therefore, γ-Al_2O_3 with a high content of strong Lewis acid sites is used as an industrial catalyst for the skeletal isomerization of n-butenes to 2-methylpropene [12], and it is important to increase its activity [11,12]. For this purpose, chemical modification of γ-Al_2O_3 with oxides by tungsten and boron was carried out [13–16]. However, with an increase in the acidity and conversion of n-butenes, the selectivity to 2-methylpropene is reduced and catalyst surface coking occurs [14]. This is associated with a change in the structure and strength of acid sites during chemical modification. The problem can be solved by increasing the concentration of acid centers γ-Al_2O_3 without using promoters.

Several researches [2] developed a number of methods for controlling the acid properties of the γ-Al_2O_3 surface through the chemical modification and heat treatment, and showed the mechanism of their action. Another new method of acid properties modifying of surface alumina is hydrothermal treatment (HTT) with the calcination to follow: the γ-Al_2O_3 hydration into boehmite proceeds in the hydrothermal conditions, and it is then converted back to oxide with improved catalytic characteristics in results of heating [4–6]. For example, we showed the positive effect of HTT support on the catalytic properties of synthesized alumoplatinum catalysts in the dehydrogenation of propane [4] and of NiMo/γ-Al_2O_3 in the hydrogenation of quinoline [9].

Unfortunately, at the present time in the literature there is no unambiguous opinion on the process of changing the acidity of the alumina support as a product of the γ-Al_2O_3 HTT. In [4–6,9], an increase in the content of Lewis acid sites after HTT is shown. However, the causes and mechanism of acidity growth were not revealed - the authors attribute the results to the formation of a large boehmite, the particles of which have the form of plates [6]. This assumption contradicts the data of [10,11], according to which the boehmite is better crystallized, and the lower is the acidity of γ-Al_2O_3 obtained from it. On the other hand, HTT removes microimpurities of Na, Fe oxides from the alumina. This can also be the reason for the increase in the content of acid sites and their strength [2]. It is probable that hydrothermal modification can increase the acidity of γ-Al_2O_3 by changing its microstructure and/or as a result of the effect of purification from metal oxides.

The purpose of this research work is investigation of the effect of hydrothermal treatment γ-Al_2O_3 on its acid properties and catalytic

* Corresponding author at: Key Laboratory of Sorbate and Catalytic Process, Alexander Butlerov Institute of Chemistry, Kazan Federal University, Kazan, 420008, Russian Federation.
E-mail address: Svetlana.Egorova@kpfu.ru (S.R. Egorova).

https://doi.org/10.1016/j.apcata.2018.01.024
Received 8 August 2017; Received in revised form 16 January 2018; Accepted 24 January 2018
Available online 04 February 2018
0926-860X/

activity in the skeletal isomerization reaction of n-butenes.

2. Materials and methods

2.1. Preparation of initial alumina and its hydrothermal treatment

Sample aluminum oxide (AO) was obtained by calcinations of high-purity pseudoboehmite Pural SB (molded with distilled water to cylindrical extrudates, d = 4 mm) manufactured by SASOL company. It contained the following microimpurities (g/ton): SiO_2 < 120; Fe_2O_3 < 100; CaO < 50; MgO < 50; Na_2O < 20; K_2O < 20; Ni,Co, Cr, Pb, Mn, Zn < 100. The hydrothermal treatment of aluminum oxide extrudates was performed in stainless steel autoclave (V = 100 ml, without stirring) at 150 °C and heating/cooling rate of 7 °C/min. An AO to water mass ratio was 1:5. On being kept for a certain time, the autoclave was cooled to room temperature and the sample was extracted, and dried at 120 °C for 2 h.

2.2. Methods of research

Thermogravimetric analysis was performed with a STA-449C (Netzsch, Selb, Germany) combined thermogravimetric and differential scanning calorimetric (DSC) analyzer coupled with an Aeolos QMS 403 quadruple mass spectrometer (Netzsch, Selb, Germany) in a temperature range of 30–1000 °C at a heating rate of 10 °C/min in a flow of argon. The concentrations of aluminum hydroxide phases were calculated from the amount of water released in their dehydration.

Electron-microscopy studies were performed at the Electron Microscopy Center of Kazan Federal University. Micrographs of the samples were obtained with a Zeiss EVO-50XVP scanning electron microscope (SEM) and with Hitachi HT7700 Excellence transmission electron microscope (TEM) operating at 80 keV.

Powder X-ray diffraction measurements were carried out using a Shimadzu XRD-7000 diffractometer with long-wavelength CuKα radiation and graphite monochromator. The range of 2θ angles was 5°–90° with a step of 0.05°. 2 to 100° with a step of 0.02° and exposure time at each point of 0.24 s without sample rotation. The coherent scattering region (CSR) sizes $D_{(hkl)}$ were calculated using the Scherrer Eq. (1).

$$D_{(hkl)} = K\cdot\lambda/(\beta\cdot\cos\theta) \quad (1)$$

which is limited by the uncertainties in K, the crystallite shape factor, and β, which is the pure diffraction broadening. Diffraction intensities were measured by scanning from 20 to 80° (2θ) with a step size of 0.02° (2θ). The error in determining the CSR size was about 10%.

The porous structure of the samples was studied by the method of low-temperature adsorption of nitrogen with a Quantachrome Autosorb IQ instrument. The adsorption isotherms of nitrogen were obtained at a temperature of −196 °C, the degassing was performed at 150 °C to a residual pressure of 10^{-4} mmHg. Specific surface area (S) was calculated according to the Brunauer-Emmett-Teller method. The pore diameter distribution was calculated by the desorption branch of isotherm using the standard Barrett–Joyner–Halenda method.

The infrared spectrum has been determined for pyridine adsorbed on acidic solids. Experiments were performed using a Bruker Vertex 70 FTIR spectrometer fitted with a mercury–cadmium–telluride (MCT) detector. The measurements were done in transmission mode using a Harrick high-temperature cell. For the FTIR analysis a sample of γ-alumina was prepared in a tablet-shape of 20 mg; its optical density was 20 mg/cm^2. Background spectrum was recorded post-activation at T = 723 K and residual pressure of less than 10^{-3} mbar. Pyridine was dosed onto the catalyst at T = 320 K. Excess of pyridine was evacuated at the same temperature.

EPR measurements were done using commercial BrukerElexsys E 580 X-band (9.6 GHz) machine. For the quantitative measurements, toluene solution of Cu-DETC complex with 4.8(2)*1016 spins per sample was used as a reference. The modeling of EPR spectra and decomposition procedure were done by EasySpin toolbox for MATLAB [12,13].

2.3. Catalytic testing

The catalytic activity of the samples in the course of n-butenes skeletal isomerization was tested in an isothermal flow-through laboratory reactor in the continuous mode at a temperature of 540 °C, gas hourly space velocity (GHSV = Reactant Gas Flow Rate/Reactor Volume) of 200 h^{-1}, raw material to steam ratio of 1:4, and charged volume of the catalyst of 20 cm^3 (13 g, see also Fig. 1S, Supplementary Information). The composition of the starting reaction mixture (n-butenes) and reaction products was analyzed with a Khromos GKh-1000 automated chromatographic complex with heat-conductivity (chromatographic column 8 m with diameter 2.5 mm, phases are brick calcined at 800 °C and 30% of pentaerythritol tetrabutyrate) and flame-ionization detectors (capillary column CP-Al_2O_3/KCl, 25 m, 0.32 mm). The attainment of the steady state by the process was judged from three repeated results of analyses of the contact gas, the error in determining concentrations of components was about 0,5% (relative). The conversion X (%) and selectivity S (%) obtained in the steady state were calculated by the formulas (2) and (3).

$$X = [(\sum N_{n-butenes\ in\ feed} - \sum N_{n-butenes\ in\ contact\ gas})/\sum N_{n-butenes\ in\ feed}]\cdot 100\,\% \quad (2)$$

$$S = [N_{isobutene}/(\sum N_{n-butenes\ in\ feed} - \sum N_{n-butenes\ in\ contact\ gas})]\cdot 100\,\% \quad (3)$$

The error in determining conversion and selectivity was about 1% (relative).

3. Results and discussion

3.1. Properties of the initial γ-Al_2O_3

The initial alumina sample was produced by calcination (550 °C,

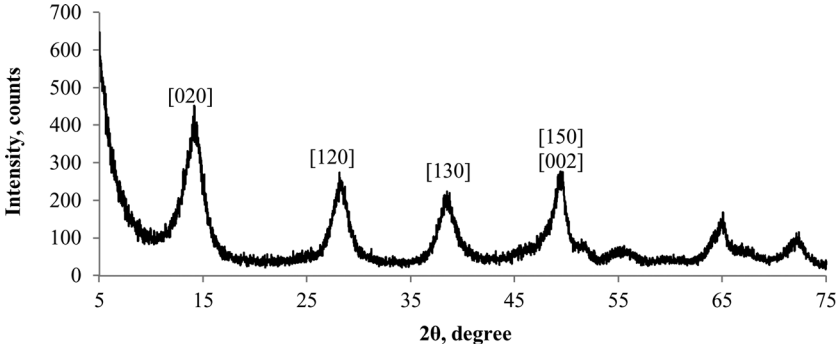

Fig. 1. Diffractogram of a Pural SB sample.

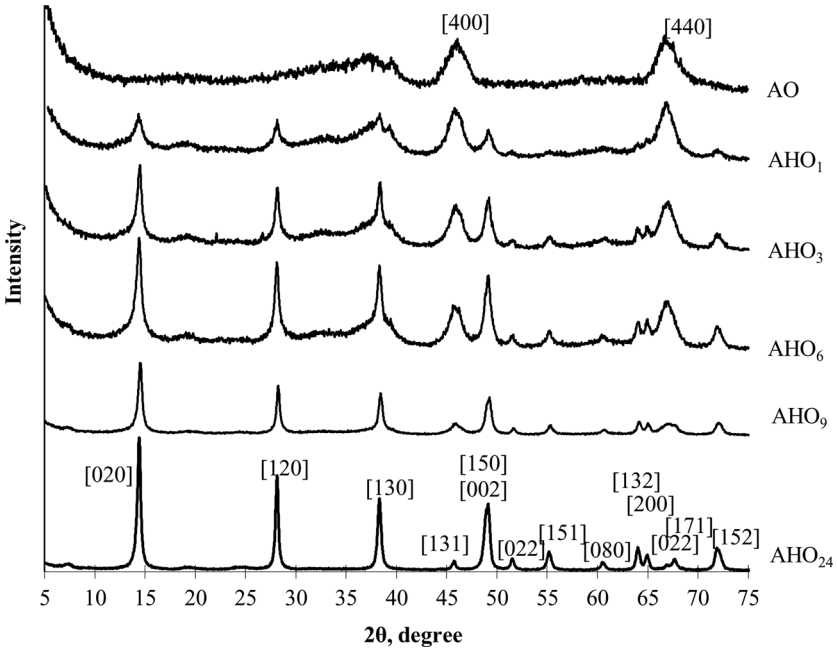

Fig. 2. Diffractograms of the samples after HTT alumina for 1–24 h.

4 h) of pseudoboehmite extrudates of Pural SB grade, obtained by alcohol technology. Results of X-ray phase analysis (Fig. 1) showing that it is a pseudoboehmite, with an average size of the coherent scattering region (CSR) of crystallites 0.52 nm along the (120) plane. We chose Pural SB due to its high purity which allows to exclude the influence of microimpurities on the acid and catalytic properties of alumina. The γ-Al_2O_3 formed during the ignition (AO, Fig. 2) is characterized by the mean CSR sizes by (400) and (440) −5.7 and 6.0 nm, respectively.

A preliminary study showed that during the heat treatment of pseudoboehmite (550 °C, 3 h) 10–15 % of the X-ray amorphous product mass is formed. A wide endothermic effect with a peak of 466 °C (phase transformation of γ-AlOOH → γ-Al_2O_3) and a shoulder in the range 213–390 °C is observed on the DSC Pural SB curve (Fig. 3), which is a result of the decomposition of partially hydrolyzed aluminum alcoholates (0.1 wt%). Heat treatment in air at 300 °C leads to the disappearance of the peak shoulder on the DSC curve (see also Fig. 4S, Supplementary Information) with a decrease in the carbon content to 0.02 wt%, while the formation of γ-Al_2O_3 is not seen on the diffractogram (see also Fig. 3S, Supplementary Information), and there is no signal of tetrahedral coordinated aluminum in the ^{27}Al NMR spectrum (see also Fig 5S, Supplementary Information).

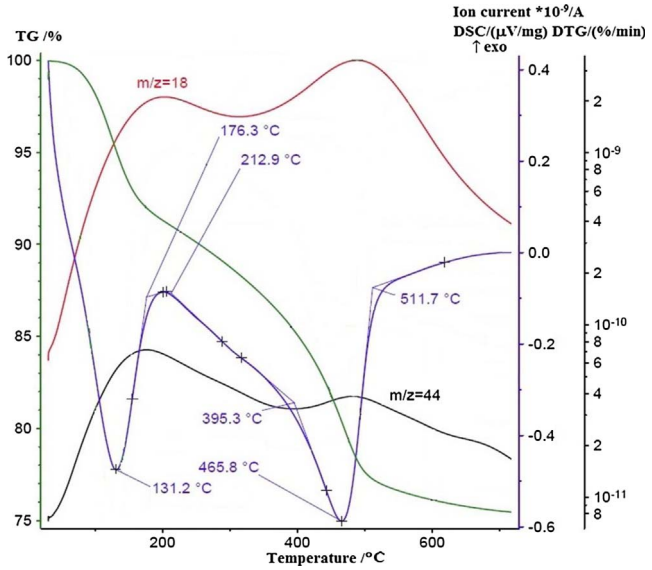

Fig. 3. TG/DSC/MS pseudoboehmite analysis of Pural SB results.

Similar low-temperature (210–350 °C) endothermic effects on the DSC curve were also found on pseudoboehmite samples obtained by neutralizing the solution of aluminum nitrate [17–20], which is due to the presence of basic aluminum salts and the formation of fine-crystalline γ-AlOOH. The more crystallized phase-homogeneous aluminum monohydroxide (boehmite) can be obtained, for example, by hydrothermal synthesis [8,11]. However, in terms of the content of acid sites of all types, aluminum oxide obtained from it is noticeably inferior to that obtained from pseudoboehmite.

γ-Al_2O_3 (AO) obtained of heat treated pseudoboehmite extrudates Pural SB (550 °C, 3 h) with an admixture of the X-ray amorphous product were used as a precursor for hydrothermal modification in order to increase the content of acid sites and catalyst activity in the skeletal isomerization of n-butenes. We conducted a series of experiments at 150 °C and P = 0.4 MPa with the duration of 1–24 h. The samples were labeled according to the Scheme Scheme 1:where AHO_x are the products of hydrothermal processing, AO_x are corresponding aluminas after calcination (550 °C, 3 h); 'x' is duration of HTT in hours.

3.2. Phase transformations during the HTT process

During the HTT with an induction period of 60 min the γ-Al_2O_3 → γ-AlOOH (boehmite) phase transition proceeds as evidenced by the appearance of lines at 2θ ≈ 14°; 28°; 38°; 49° which correspond to boehmite (Fig. 1and Figure 3). After 1 h of HTT the mass loss from the TG/DSC results in the range 390–510 °C corresponds to the formation of 29 wt% boehmite. This may be the result of crystallization in boehmite (Bm) of the X-ray amorphous component of AO, as the most reactive fragment of the starting oxide. A further increase of the HTT duration up to 24 h results in a linear increase in Bm content up to 100% (Fig. 4). The structure of the resulting boehmite is being improved as evidenced by the increase in the average CSR size and the maximum dehydration of Bm into γ-Al_2O_3 on the DSC curve (Fig. 4).

In the SEM and TEM images (Fig. 5) the formation of boehmite particles of two types is observed.

The first are formed on the outer surface of granules and macropores at short HTT times (1–3 h) in the form of needles with a length of ≈150 nm and a cross section of ≈15–20 nm (Fig. 5a–d), and are

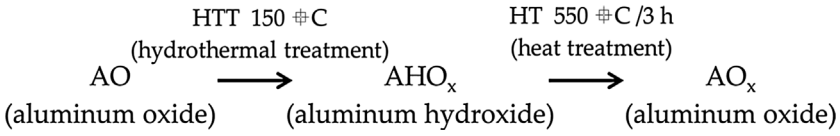

Scheme 1. Successive hydrothermal and heat treatment of alumina.

transformed into plates and parallelepipeds during the HTT (there are not such particles in the initial AO).

According to the Fig. 5a–d, the volume of granules of HTT products is identified by small almost spherical particles of 15–17 nm which grow slowly predominantly in one direction up to 100 nm in the form of needles with a cross section of 15–17 nm with an increase in the HTT duration of more than 6-9 h. Taking into account the step-like nature of the change in the average CSR size, the values of the peak of the temperature dehydration of Bm in γ-Al_2O_3 (Fig. 4) as well as the results of SEM and TEM (Fig. 5), it can be assumed that the phase transformation in HTT proceeds in two stages with successive formation of two types of boehmite particles (**Bm1** and **Bm2**) according to the scheme shown in Fig. 6.

The starting γ-Al_2O_3 contains a certain amount of the X-ray amorphous product (10–15 wt%), which under HTT conditions is primarily undergone to conversion to boehmite which transformed from "needles"to plates and parallelepipeds during processing. This process is due to the implementation of the "dissolution-precipitation" mechanism: formed water- and hydroxo- complexes of aluminum formed during dissolution are directed to crystallize along the c axis (Fig. 7).

The formation of needle-like fragments in the granule volume happens only after the longer HTT duration which is probably due to the steric factors. The phase transition γ-Al_2O_3 → γ-AlOOH locally proceeds, and the macrostructure of the granules persists.

3.3. Parameters of porous system of AHO_x and AO_x

Change in the phase composition affects the texture characteristics of the samples (Table 1).

The value of specific surface area varies extremely with the HTT duration reaching a maximum during the third hour. The initial increase is due to the formation of a new phase of boehmite in the macropores, and after it a further decrease is due to the enlargement of the boehmite formed. The average pore diameter practically does not change during the first 3 h of treatment, and then it increases which is explained by the processes of γ-Al_2O_3 phase transformation into boehmite and the growth of crystals of the latter, which are shown on Fig. 7. A similar dependence of the specific surface area on the HTT duration is also observed for AO_x samples (Table 1).

3.4. Acidic properties of synthesized samples γ-Al_2O_3

We studied the acid properties of experimental AO_x samples by the methods of adsorbed pyridine probe IR-spectroscopy and EPR-spectroscopy of adsorbed anthraquinone. These probes are used to study the Lewis acid sites (LAS) [2,12,13]. The results of the AO-AO_{24} series analysis by adsorbed pyridine IR-spectroscopy are presented in Table 2 (see also Fig. 6S, Supplementary Information). Dependence of the LAS amount in alumina obtained by calcination of HTT products is extreme with a maximum during the third hour of HTT. At short treatment times (1–3 hours) the content of all LAS increases, then (after 6-24 h) it decreases monotonically.

The using of EPR-spectroscopy to analyze the acid properties of the γ-Al_2O_3 surface allows one to identify the strong LAS (adsorption band of pyridine = 1623 cm^{-1} [12–14]) which are pairwise located aluminum cations at a distance ≈5.8 Å localized on the (110) plane of γ-Al_2O_3. The precursor of which is the (010) plane of the boehmite formed (Fig. 7). The results of quantitative measurements for AO_x samples are shown in Table 2 (see also Fig. 6S, Supplementary Information). In a series of AO-AO_{24} samples the values obtained pass through a maximum for AO_3, similar to the results of IR-spectroscopy of adsorbed pyridine. We can assume that the number of fragments representing strong LAS localized on the forming γ-Al_2O_3 (110) plane increases at the HTT at small times process and for long periods due to its "completion" is reduced.

3.5. Catalytic tests of synthesized γ-Al_2O_3 samples in the reaction of n-butenes skeletal isomerization

The results of catalytic testing of the samples after HTT and calcination are shown in Table 3.

As an example (Fig. 8), it is showed the catalytic performance of sample AO_3 with time on stream. The conversion of n-butenes (X) dependence on the HTT duration passes through a maximum: it increases after HTT at small times, and then begins to decrease. A comparison of the catalytic tests results and quantitative acidity measurements shows a correlation between the conversion of n-butenes and the content of strong LAS from the adsorbed anthraquinone EPR-spectroscopy (R_2 = 0.96). According to adsorbed pyridine IR-spectroscopy the best correlation (R_2 = 0.95) is of the conversion of n-butenes and strong LASs (for medium and weak R_2 - 0.88 and 0.11 respectively).

An increase in the content of isobutylene in the contact gas (AO_1-AO_6) is accompanied by a slight rise in the concentrations of C_3 and C_{5+} hydrocarbons. Formation of the latter is a consequence of successive reactions of butenes dimers and cracking of products [11] to the Scheme Scheme 2.

Since the formation of 2-methylpropene and by-products C_3, C_{5+} occurs at the same centers an increase in the activity of γ-Al_2O_3 in the skeletal isomerization of n-butenes is accompanied by an acceleration of the above-mentioned side reactions.

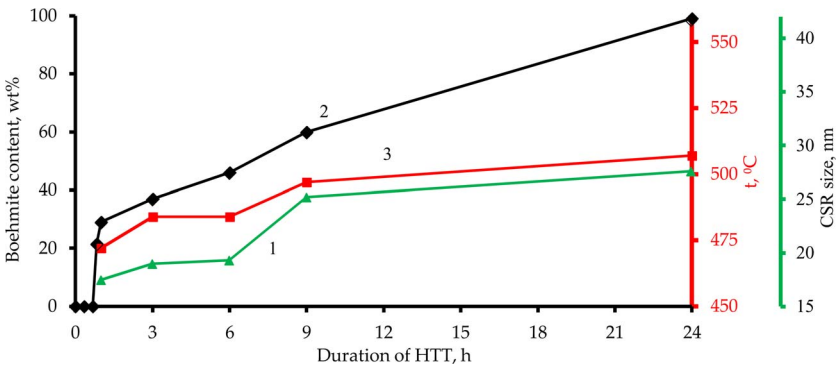

Fig. 4. Dependences of the average size of CSR (on (120) plate) boehmite (1), its content (2) and the maximum dehydration in γ-Al_2O_3 (3) from the duration of HTT.

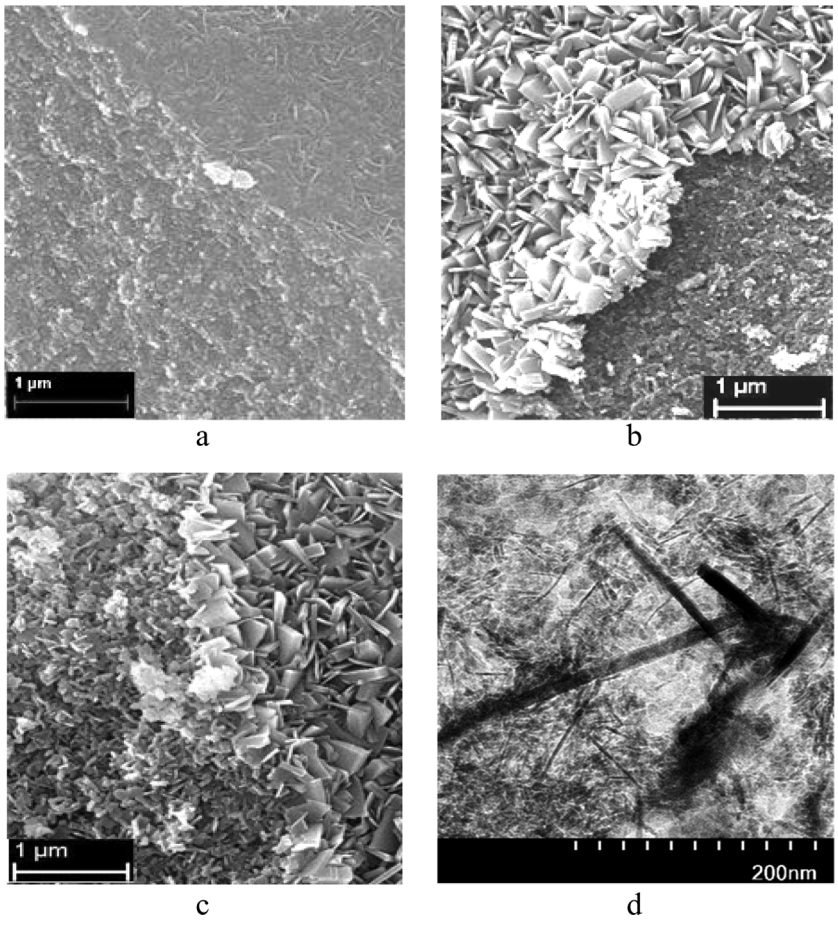

Fig. 5. Particles on the surface and the chips of granules. SEM: a – after 3 h of HTT, b – after 6 h of HTT, c – after 24 h of HTT; TEM: d – after 3 h of HTT.

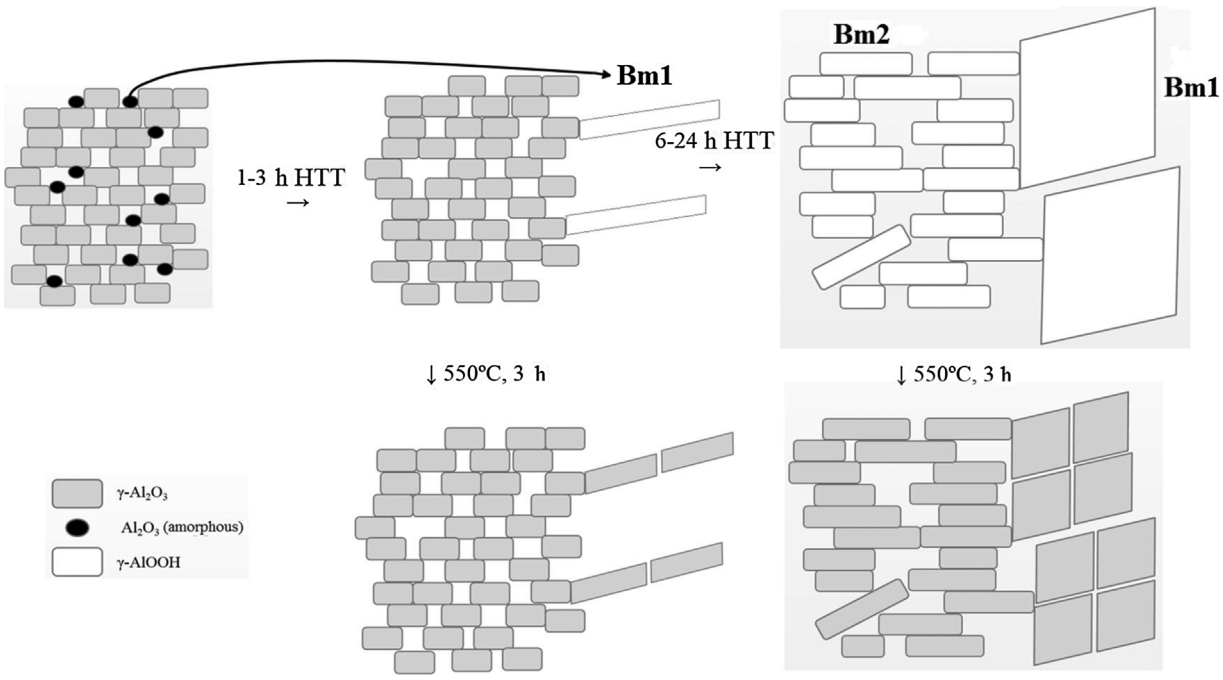

Fig. 6. Effect of HTT and subsequent heat treatment on the phase composition and structure of AO.

Table 3 shows that the growth of catalytic activity is observed up to 3 h of treatment at the stage of formation of Bm1 from the X-ray amorphous constituent of the initial alumina (AO). The formation of Bm2 at longer treatment times (> 3 h) and the improvement in the structure of Bm1 and Bm2 are accompanied by a decrease of catalytic activity. Probably, an increase in the activity of the catalyst is due to the formation of Bm1.

A comparison of the catalytic tests results and quantitative acidity

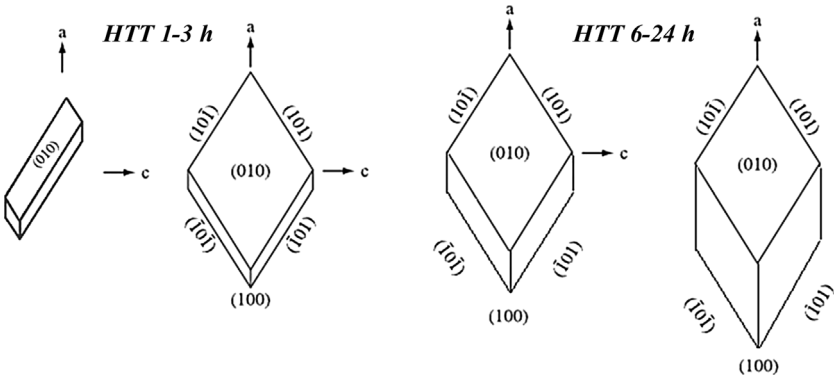

Fig. 7. Diagram of growth of primary boehmite particles under the hydrothermal conditions.

Table 1
The results of the analysis of experimental samples by the method of low-temperature nitrogen adsorption (see also Fig. 2S, Supplementary Information).

Sample	Specific surface area (m^2/g)	Pore volume (cm^3/g)	Average pore diameter (nm)
AO	199	0.68	9.8
AHO_1	220	0.65	9.7
AHO_3	225	0.61	9.7
AHO_6	191	0.61	10.0
AHO_9	160	0.58	12.2
AHO_{24}	91	0.54	20.0
AO_1	221	0.64	9.8
AO_3	230	0.60	9.7
AO_6	205	0.58	10.5
AO_9	184	0.56	12.5
AO_{24}	161	0.54	15.0-40.0

measurements shows a correlation between the conversion of n-butenes and the content of strong LAS from the adsorbed anthraquinone EPR-spectroscopy ($R^2 = 0.96$) and the adsorbed pyridine IR-spectroscopy ($R^2 = 0.95$).

The main side process in the skeletal isomerization of n-butylenes to isobutylene is oligomerization of butenes (cracking of which results in C_3 and C_5 hydrocarbons detected in the contact gas / reaction products). It is isobutylene is more inclined (reactive) to the formation of oligomers. These processes can be considered as a sequential scheme for the formation of by-products. Therefore, with the intensification of the first stage namely the skeletal isomerization of n-butylenes the formation of by-products in general is intensified. Accordingly, for selectivity AO, which are more active in skeletal isomerization, the selectivity is somewhat reduced (Table 3). Thus, the growth of the catalytic activity of AO_1-AO_6 samples is a consequence of an increase in the content of strong LAS which are identified as strongly paired centers (located at a distance of no more than 6 Å from each other [12,14]) localized predominantly on the (110) plane. It should be also noted that the direct dependence of acidity (Table 2) or catalytic indexes (Table 3) of the specific surface (Table 1) is not observed. Thus, samples AO_6 and AO_9 characterized by a lower specific surface area compared to AO contain more acid sites than initial AO and they are more active in the skeletal isomerization reaction of n-butenes.

4. Conclusion

Hydrothermal modification of the alumina catalyst for the skeletal isomerization of n-butenes was studied. The presence of the X-ray amorphous component in the initial aluminum oxide during the hydrothermal treatment causes the formation of two types of boehmite from different particle morphologies. The particles of boehmite in the form of needles of 10–15 nm diameter and 100–300 nm length are formed on the outer surface of the granule and macropores (> 1 μm) up to 3 h of hydrothermal treatment (150 °C) by the "dissolution-precipitation" mechanism from the X-ray amorphous component. This product forms γ-Al_2O_3 with high acidity at calcination (550 °C, 3h). All strong Lewis acid sites of the γ-Al_2O_3 are located in pairs at a distance of 5–6 Å on the (110) plane. The boehmite is formed at the hydrothermal treatment duration > 3 h (150 °C) from crystalline γ-Al_2O_3 in mesopores with a particle size comparable to the initial alumina ≈20 nm. At the duration of more than 3 h (150 °C) both structures of boehmite are improved with a decrease in the concentration of Lewis acid sites, which leads to a decrease in the catalytic activity of the oxides in the skeletal isomerization reaction of n-butenes. Since the active centers of this reaction are strong Lewis acid sites of aluminum oxide, the method of hydrothermal modification of the catalyst containing an X-ray amorphous phase at 150 °C for 3 h can be used to obtain an effective skeletal isomerization catalyst for n-butylene based on γ-Al_2O_3.

Acknowledgements

This research is carried out under the Russian Government Program of Competitive Growth of Kazan Federal University.

Table 2
Acid properties of the samples from the results of IR-spectroscopy of adsorbed pyridine and EPR-spectroscopy of adsorbed anthraquinone.

Sample	HTT, h	Number of LAS			
		IR-spectroscopy of adsorbed pyridine (rel.[a]unit. g^{-1})			EPR- spectroscopy of adsorbed anthraquinone
		Weak (1595 cm^{-1})	Medium (1612 cm^{-1})	Strong (1623 cm^{-1})	(μmol/g)
AO	0	11	100	48	17.9
AO_1	1	28	106	59	–
AO_3	3	29	109	61	23.8
AO_6	6	29	104	58	–
AO_9	9	29	96	55	20.2
AO_{24}	24	27	77	37	15.8

[a] for 100 rel. units the content of mean LAS in the original AO.

Table 3
Results of catalytic tests of a series of samples obtained as by HTT at 150 °C and subsequent calcination (AO_x) in the skeletal isomerization reaction of n-butenes.[a]

Sample	X / S	Hydrocarbon components of contact gas[b](% vol.)					
	(% / %)	C_3H_6	iso-C_4H_{10}	n-C_4H_{10}	n-C_4H_8	iso-C_4H_8	≥C_5
Initial fraction	–	0.3	0.8	7.6	89.9	0.8	0.6
AO	29/88	2.2	0.7	6.7	64.3	24.2	1.2
AO_1	31/86	2.3	0.7	6.7	62.7	24.5	1.3
AO_3	33/86	2.3	0.6	6.7	62.1	25.0	1.3
AO_6	32/86	2.3	0.7	6.7	62.3	24.8	1.3
AO_9	30/88	2.2	0.6	6.7	66.0	24.3	1.3
AO_{24}	25/90	2.1	0.6	6.7	68.7	19.9	1.2

[a] The samples was tested in an isothermal flow-through laboratory reactor in the continuous mode at a temperature of 540 °C, gas hourly space velocity (GHSV = Reactant Gas Flow Rate/Reactor Volume) of 200 h^{-1}, raw material to steam ratio of 1:4, and charged volume of the catalyst of 20 cm^3(13 g), time on stream 8–100 h.
[b] for contact gas of all sample: C(H_2) = 0.1; C(C_1-C_3) = 0.4; C(CO_2) = 0.4.

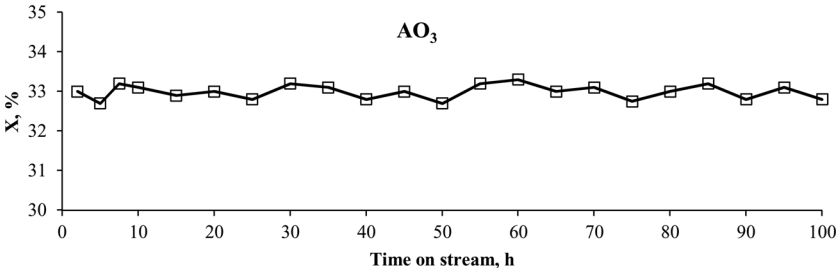

Fig. 8. Variation the catalytic conversion of n-butenes with time on stream for sample AO_3.

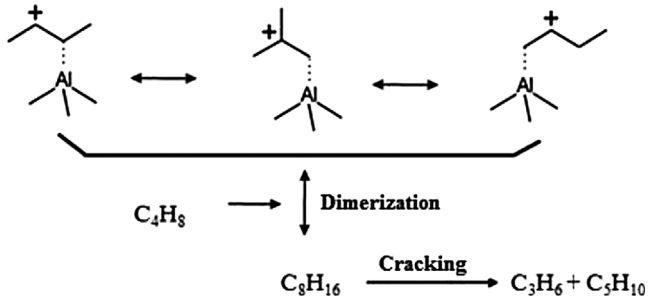

Scheme 2. Formation butenes dimers and cracking of products in the of n-butenes skeletal isomerization.

The thermal analysis of samples was carried out at the Federal Center for Collective Use of the Kazan Federal University with the support of the Russian Agency for Science and Innovation A.V. Gerasimov.

The scanning electron microscopy and transmission electron microscopy measurements were performed at the Interdisciplinary Center "Analytical Microscopy" of the Kazan Federal University V.V. Vorobiev and V.G. Evtyugin respectively.

Appendix A. Supplementary data

Supplementary material related to this article can be found, in the online version, at doi:https://doi.org/10.1016/j.apcata.2018.01.024.

References

[1] M. Trueba, S.P. Trasatti, Eur. J. Inorg. Chem. (2005) 3393–3403.
[2] H. Pines, W.O. Haag, J. Amer, Chem. Soc. 10 (1960) 2471–2483.
[3] E.A. Paukshtis, E.N. Yurchenko, Russ. Chem. Rev. 52 (1983) 242–258.
[4] R.M. Mironenko, O.B. Belskaya, V.P. Talsi, T.I. Gulyaeva, M.O. Kazakov, A.I. Nizovskii, A.V. Kalinkin, V.I. Bukhtiyarov, A.V. Lavrenov, V.A. Likholobov, Appl. Catal. A 469 (2014) 472–482.
[5] G. Li, Y. Liu, Z. Tang, C. Liu, Appl. Catal. A 437–438 (2012) 79–80.
[6] L. Jun-Cheng, X. Lan, X. Feng, W. Zhan-Wen, W. Fei, Appl. Surf. Sci. 253 (2006) 766–770.
[7] A.S. Ivanova, E.V. Kul'ko, O.V. Klimov, G.A. Bukhtiyarova, G.S. Litvak, A.A. Budneva, E.A. Paukshtis, D.A. Zyuzin, E.M. Moroz, V.I. Zaikovskii, A.S. Noskov, Kinet. Catal. 49 (2008) 791–801.
[8] P.S. Santos, A.C.V. Coelho, H.S. Santos, P.K. Kiyohara, Mater. Res. 12 (2009) 437–445.
[9] A.A. Lamberov, E.Y. Sitnikova, I.N. Mukhambetov, R.F. Zalyaliev, R.R. Gilmullin, K.K. Gilmanov, Catal. Ind. 4 (2012) 141–149.
[10] P. Nortier, P. Fourre, A.B.M. Saad, O. Saur, J.C. Lavalley, A.B. Mohammed, J.C. Lavalley, A.B.M. Saad, O. Saur, J.C. Lavalley, Appl. Catal. 61 (1990) 141–160.
[11] S. Van Donk, J.H. Bitter, K.P. De Jong, Appl. Catal., A 212 (2001) 97–116.
[12] A.A. Lamberov, I.N. Mukhambetov, R.F. Zalyaliev, Catal. Ind. 6 (2014) 128–133.
[13] L. Gielgens, J. Catal. 154 (1995) 201–207.
[14] S. Meijers, J. Catal. 156 (1995) 147–153.
[15] A.A. Lamberov, E.Y. Sitnikova, R.R. Gilmullin, N.A. Sidorov, Catal. Ind. 3 (2010) 55–62.
[16] E.V. Kul'ko, A.S. Ivanova, A.A. Budneva, E.A. Paukshtis, Kinet. Catal. 46 (2005) 132–137.
[17] G. Castruita, Y.A. Perera-Mercado, E.M. Saucedo-Salazar, J. Inorg, Organomet. Polym. 23 (2013) 1145–1152.
[18] I.N. Mukhambetov, A.A. Lamberov, B.V. Yavkin, M.R. Gafurov, G.V. Mamin, S.B. Orlinskii, J. Phys. Chem. 118 (2014) 14998–15003.
[19] M.R. Gafurov, I.N. Mukhambetov, B.V. Yavkin, G.V. Mamin, A.A. Lamberov, S.B. Orlinskii, J. Phys. Chem. 119 (2015) 27410–27415.
[20] E.V. Lunina, M.N. Zacharova, G.L. Markaryan, A.V. Fionov, Colloids Surf. A 115 (1996) 195–206.